JACS
JOURNAL OF THE AMERICAN CHEMICAL SOCIETY

Article

Efficient and Rapid Mechanochemical Assembly of Platinum(II) Squares for Guanine Quadruplex Targeting

Amine Garci, Katherine J. Castor, Johans J. Fakhoury, Jean-Louis Do, Justin Di Trani, Robin S. Stein, Anthony K. Mittermaier, Tomislav Friscic, and Hanadi F. Sleiman

J. Am. Chem. Soc., **Just Accepted Manuscript** • DOI: 10.1021/jacs.7b09819 • Publication Date (Web): 23 Oct 2017

ACS Publications

Journal of the American Chemical Society is published by the American Chemical Society. 1155 Sixteenth Street N.W., Washington, DC 20036

Efficient and Rapid Mechanochemical Assembly of Platinum(II) Squares for Guanine Quadruplex Targeting

Amine Garci, Katherine J. Castor, Johans Fakhoury, Jean-Louis Do, Justin Di Trani, Robin S. Stein, Anthony K. Mittermaier, Tomislav Friščić* and Hanadi Sleiman*

Department of Chemistry, McGill University, 801 Sherbrooke Street West, Montréal, Québec, Canada H3A 0B8; Co-corresponding authors: tomislav.friscic@mcgill.ca and hanadi.sleiman@mcgill.ca

Abstract

We present a rapid and efficient method to generate a family of platinum supramolecular square complexes, including previously inaccessible targets, through the use of ball milling mechanochemistry. This one-pot, two-step process occurs in minutes and enables the synthesis of the squares $[Pt_4(en)_4(N\cap N)_4][CF_3SO_3]_8$ (en= ethylenediamine, N∩N = 4,4'-bipyridine derivatives) from commercially available precursor K_2PtCl_4 in good to excellent yields. In contrast, solution-based assembly requires heating the reagents for weeks and gives lower yields. Mechanistic investigations into this remarkable rate acceleration revealed that solution-based assembly (refluxing for days) results in the formation of large oligomeric side-products that are difficult to break down into the desired squares. On the other hand, ball milling in the solid state is rapid and appears to involve smaller intermediates. We examined the binding of the new supramolecular squares to guanine quadruplexes, including oncogene and telomere-associated DNA and RNA sequences. Submicromolar binding affinities were obtained by fluorescence displacement assays (FID) and isothermal titration calorimetry (ITC), with binding preference to telomere RNA (TERRA) sequences. ITC showed a 1:1 binding stoichiometry of the

metallosquare to TERRA, while the stoichiometry was more complex for telomeric quadruplex DNA and a double-stranded DNA control.

Introduction

Coordination-driven self-assembly is a highly efficient approach to create a range of molecular architectures, with applications from biomedical to materials sciences.[1] The most common strategies in this area typically employ kinetically labile transition metal complexes, and rely on error-correction provided by reversible assembly to reach the thermodynamically favored product.[2] However, these approaches are limited by the inherent lability of the final metallosupramolecular product, as well as by its structural sensitivity to different environments, for example in biomedical applications. Using more inert transition metal complexes leads to robust assemblies, but often requires heating to labilize the metal-ligand bonds and steer the system away from kinetically trapped side-products.[3] However, this is not always possible, and often low reaction yields are obtained. The use of high temperature may also be problematic when the entropy of product formation is negative, as it accentuates the entropic contribution to free energy and opposes enthalpic gain from product formation. Supramolecular assemblies based on Pd(II) and Pt(II) are a case in point for these observations; these complexes have been extensively studied for their molecular recognition, catalysis,[4] sensing,[5] antitumor activity,[6] drug encapsulation,[7] lipid bilayer channel formation,[8] and optoelectronic properties.[9] The first example of a discrete cationic molecular square based on Pd(II) was reported by Fujita et al., who utilized the chelating ligand ethylenediamine (**en**) as a means to direct the assembly of palladium cations and bridging 4,4'-bipyridine ligands into the structure [(en)Pd(4,4'-bipyridine)]$_4$.[10] Our interest in such supramolecular squares arises from the observation that the

more inert platinum(II) analogue of this cationic assembly can bind strongly to DNA guanine quadruplexes and inhibit the cancer-specific enzyme, telomerase.[11] However, due to the inertness of the Pt-N bond, this supramolecular square is typically synthesized by a high-temperature self-assembly process over extended periods of time, notably by exposure of the aqueous reactant mixture to 100^{o}C for 4 weeks.[12] Two elegant strategies have been explored to make well-defined architectures from platinum complexes. The first approach focuses on rigid, preorganized ligands and platinum phosphine complexes to direct self-assembly, and has resulted in an extensive range of platinum metallacycles with numerous applications.[13] The second approach, which creates water soluble complexes of Pt(II) with the **en** chelating ligand, labilizes the inert Pt(II)-pyridine bond using an excess of salt[14] or employing an external stimulus such as ultraviolet (UV) light, followed by molecularly "locking" the complexes upon removal of this stimulus.[15] This approach is complicated by extensive purification procedures when excess salts are used, and sensitivity of some ligands to UV light, thus hindering the ability to generate a large number of water-soluble platinum complexes with different functionalities.[16]

Recently, non-conventional synthetic procedures such as ultra-sonication,[17] microwave[18] and solvent-free self-assembly methods based on mechanochemical milling[19] or accelerated aging[20] have made their entry in the field of synthetic supramolecular chemistry. Mechanochemical transformations by ball milling[21] have proven particularly efficient in the assembly of a wide diversity of supramolecular architectures based on hydrogen bonds,[22] such as pharmaceutical cocrystals,[23] halogen bonds,[24] reversible covalent bond assembly,[25] as well as for the assembly of coordination polymers[23a,26] and open metal-organic frameworks.[27] Mechanochemical techniques have been shown to enable the assembly of supramolecular and covalent structures faster,[25b] with superior selectivity[28] and efficiency[29] compared to solution

techniques, while also permitting the synthesis of structures that have previously been inaccessible.[30] Examples of complex structures assembled by mechanochemical routes include large macrocyclic hosts like calix[n]arene (n=5 or 7),[31] giant hydrogen bonded capsules[32] and covalent organic-cage-based boronate esters and imine linkages.[33]

Guanine quadruplexes (G4) are DNA and RNA secondary structures formed by self-folding of four guanine bases in a planar arrangement via Hoogsteen hydrogen-bonds. The design of molecules that selectively bind to these motifs has emerged as a selective potential antitumor therapy.[34] It has been shown to inhibit the cancer-specific telomerase enzyme, and to downregulate a number of oncogenes.[35] Recent research has also focused on targeting a G-rich non-coding RNA region, known as telomeric repeat-containing RNA (TERRA).[36] TERRA is associated with many cell regulation mechanisms, including telomere maintenance and stability in both telomerase-positive and negative (ALT) cancer cells. TERRA folds into a parallel-only topology that is more stable than DNA analogues.[37] Targeting RNA G4 motifs could result in high specificity for a wide range of cancer cells. Many quadruplex binders capable of stabilizing the G4-motifs have been obtained via traditional synthetic organic and inorganic chemistry methods.[37a] The implementation of self-assembled supramolecular structures for G-quadruplex recognition is a particularly appealing strategy to create these binders. We[11] and others[38,39,40] have reported the high affinity binding of Pt(II) supramolecular squares to telomeric G-quadruplexes and telomerase inhibition. However, the investigation and development of the biomedical potential of platinum-based supramolecular squares are hindered by the low yields and long reaction times required for the assembly in dilute solutions. Therefore, we were intrigued by the 2002 report of Orita and co-workers, who described the rapid and high-yielding preparation of platinum- and palladium-based squares through mechanochemistry, specifically

by manual grinding of pre-synthesized *cis*-protected $Pt(en)(NO_3)_2$ monomeric units with 4,4'-bipyridine.[41] Following this pioneering work, however, there have been no other reports on the mechanochemical assembly of supramolecular square structures.

We now report the efficient generation of a series of new platinum metallacycles from simple Pt(II) precursors by using ball milling mechanochemistry, in good to excellent yields and high purities, and provide insight into the factors directing the mechanochemical assembly of Pt(II) squares. In particular, we present a one-pot, two-step[42] process that enables the synthesis of supramolecular squares directly from commercially available K_2PtCl_4 salt, without the need to separately prepare or isolate reactive cis-protected monomers.[43] Whereas the work of Orita and co-workers utilized manual grinding in a mortar and pestle, we show that the reactivity can be adapted to automated ball milling, a methodology that provides a significantly larger degree of control over mechanochemical reaction conditions (*e.g.* atmosphere, milling time, frequency, choice of milling media).[44] Through the use of ball milling, we have now also expanded this reactivity for rapid, high-yielding synthesis of a family of platinum(II) supramolecular squares **S1-S4** based on 4,4'-bipyridine and related bridging ligands (Scheme 1a,b). The resulting availability of diverse platinum squares enabled us to evaluate their binding affinity towards the G4-forming human telomeric, oncogene promoter KRAS and TERRA sequences by using fluorescence displacement, UV/vis spectrometry and isothermal calorimetry experiments.

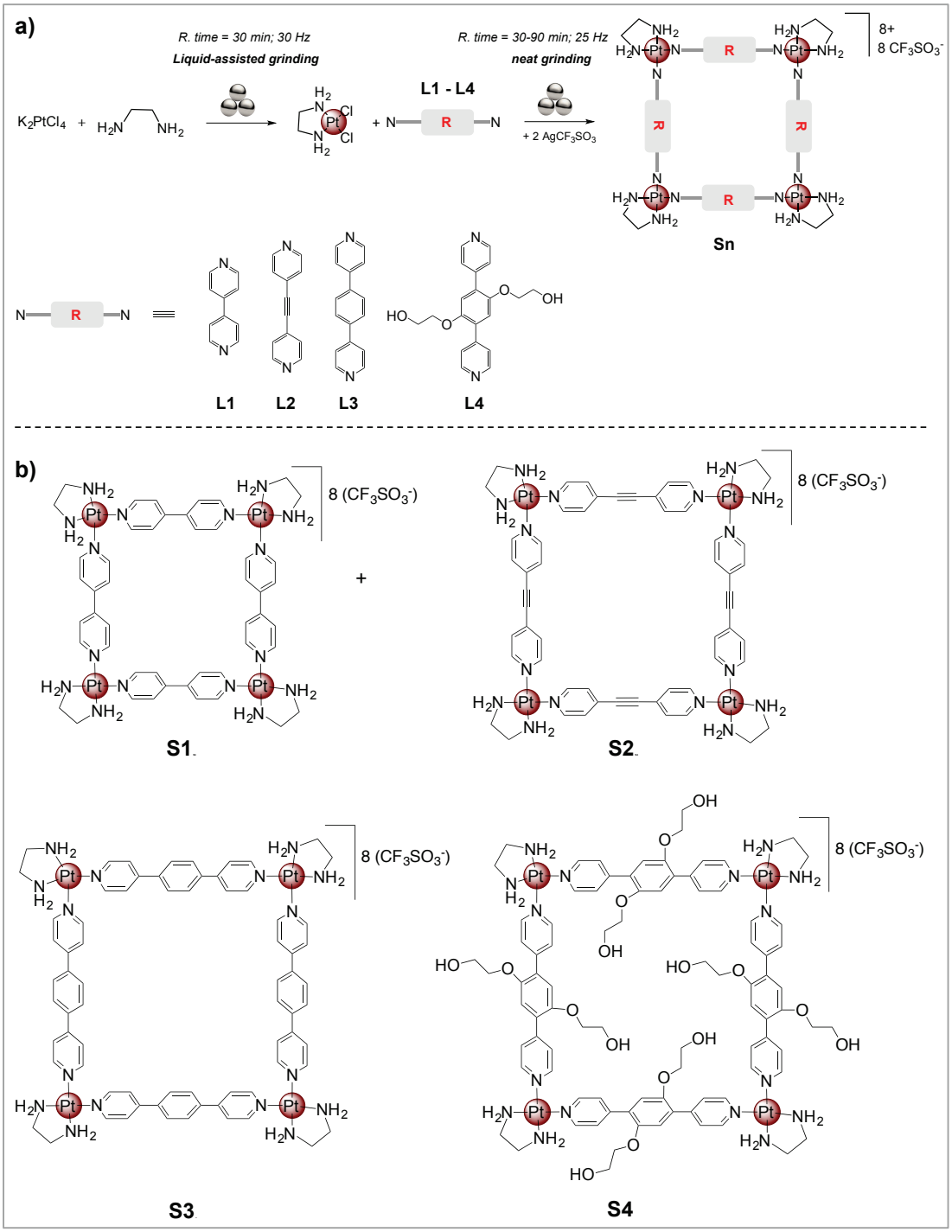

Scheme 1 a) Mechanochemical synthesis of platinum squares of the general formula $\mathbf{[Pt_4(en)_4(N \cap N)_4]}[CF_3SO_3]_8$; b) The Pt-squares **S1 (80%), S2 (53%), S3 (64%) and S4 (48%)** synthesized in this work.

Results and Discussion

Mechanochemical Procedure for the Synthesis of a Molecular Square

To facilitate the mechanochemical synthesis of platinum supramolecular squares, we focused on developing a synthetic procedure that would start from a readily available metal precursor, K_2PtCl_4. In particular, we sought to explore the ability to convert K_2PtCl_4 into the *cis*-protected platinum complex $PtenCl_2$ by mechanochemical ligand exchange with ethylenediamine (**en**), using either neat (dry) grinding or milling in the presence of a liquid additive (liquid-assisted grinding, LAG, Scheme 1a).[45] The exploration of different reaction parameters (Supporting information: sections 2 and 8) revealed that almost quantitative conversions to $PtenCl_2$ were obtained upon 30 minutes LAG of K_2PtCl_4 and **en** in a 1:1 stoichiometric ratio, in the presence of 4 equivalents of acetonitrile as a milling liquid. After separation of the byproduct KCl, the target complex $PtenCl_2$ was obtained in upwards of 80% isolated yield.

To achieve the synthesis of a molecular square from mechanochemically obtained $PtenCl_2$, we envisaged that further milling in the presence of a silver salt and the bridging bis(pyridine) ligand **L1** should lead to concomitant removal of chloride ligands to form AgCl, and the assembly of platinum(II) squares through Pt-N coordination bonds. Indeed, milling of $PtenCl_2$ in the presence of two equivalents of $AgNO_3$ and one equivalent of **L1** at a milling frequency of 25 Hz led to the formation of the targeted cationic square, identified by ^{1}H nuclear magnetic resonance (NMR) spectroscopy and mass spectrometry (MS). Specifically, the formation of the platinum(II) square was detectable in the ^{1}H NMR spectrum of the product already after 5 minutes milling through the appearance of resonances at 8.9 ppm and 7.9 ppm, ascribed to protons in α- and β-positions of the pyridine rings attached to Pt^{2+}, respectively (Figure 1a). After 60 minutes milling the ^{1}H NMR spectrum was fully consistent with that of the

expected square, indicating near-quantitative yield (Figure 1a). Importantly, the reaction outcome was affected by the choice of milling frequency: somewhat harsher milling at a frequency of 30 Hz led to the formation of the targeted square along with oligomeric byproducts (Supporting Information Figure S7).

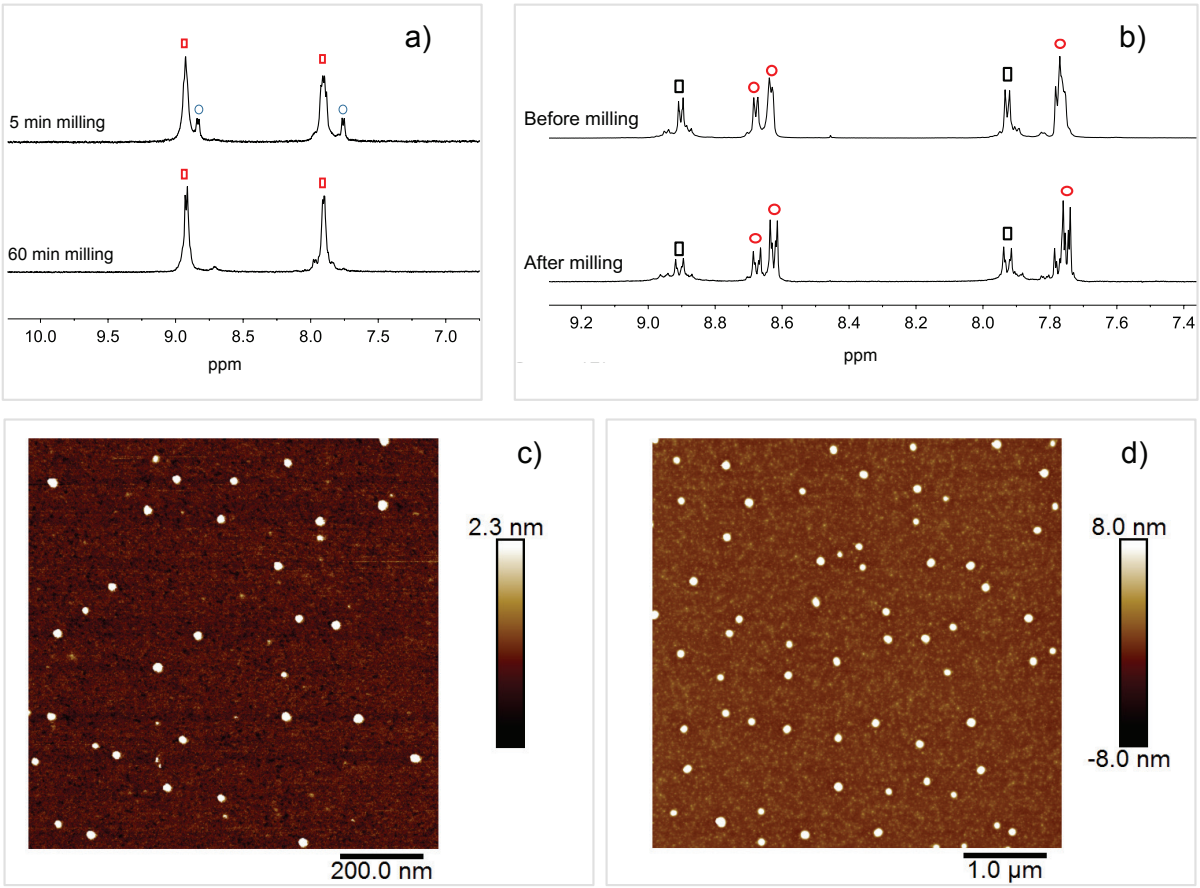

Figure 1 a) ^{1}H NMR spectra (D_2O, 23°C) of products resulting from the ball-milling synthesis of the square $[Pten(bpy)]_4$ $[NO_3]_8$: (above) after 5 min milling, showing a mixture of square **S1**(□) and oligomeric intermediate (○). (below) after 60 min milling, showing the convergence of the synthesis to the target square **S1**; b) ^{1}H NMR spectra (D_2O, 23°C) of products resulting from the solution synthesis of the square $[Pten(bpy)]_4$ $[NO_3]_8$: (above) reaction mixture after solution synthesis by refluxing for 3 days, showing square S1(■) (35%) and by-products (○). (below) the same reaction mixture after milling for 90 min at 25 Hz, showing that the byproducts do not converge to square **S1**. AFM height images: c) corresponding to the products resulting from the ball milling synthesis of the square **S1** (30 min of milling) revealing a mostly monodisperse population of spherical structures with average height 4.9 nm and width of 20.5 nm; d) corresponding to the solid sample obtained after 3 days aqueous reflux followed by evaporation revealed very different particle morphologies with average height of 17 nm and width of 104 nm.

Solution vs. mechanochemical assembly

In order to evaluate the efficiency of this mechanochemical procedure, as well as to verify whether the results of our ^{1}H NMR analysis might have been affected by spontaneous assembly of the square structure during sample work-up, we also explored the assembly of the square in aqueous solution. This was done by either refluxing pre-synthesized $Pt(en)(NO_3)_2$ in the presence of ligand **L1** for 3 days, or by stirring at room temperature for 7 days. In contrast to room-temperature milling experiments, stirring an aqueous solution of $Pt(en)(NO_3)_2$ with 4,4'-bipyridine at room temperature did not lead to the formation of molecular squares, indicating that our evaluation of square formation by milling was not affected by aqueous sample work-up. The much harsher reflux conditions gave a maximum of 35% of the square along with byproducts (Figure 1b, top). Similar results were also obtained upon attempted assembly of the square in methanol solution (Supporting Information, section 10, for NMR monitoring of the room temperature reaction in methanol).

The comparison of mechanochemical self-assembly to that in aqueous solution reveals remarkable speed and efficiency for the mechanochemical process. In order to explore whether the reaction efficiency might have been affected by the presence of Ag^+ ions we performed a control experiment in which we prepared $enPt(NO_3)_2$ by reaction of $enPtCl_2$ with $AgNO_3$ followed by removal of the silver salt, and milling for 90 minutes with **L1**. In this case as well, the clean formation of the platinum square was observed, indicating that the silver ions do not play a major role in the rate acceleration upon ball milling (Supporting Information Figure S10). Moreover, the mechanochemical synthesis was also possible using silver triflate (AgO_3SCF_3) as the silver salt, indicating that choice of anion was not critical for the square **S1** assembly.

Consequently, we speculate that the significantly higher rate of square formation through ball milling, rather than in solution, is associated with the absence of bulk solvent, enabling the self-assembly process to take place between highly concentrated reactant phases.

Mechanistic Insight from Intermediates and Byproducts Analysis

The differences between solution and mechanochemical environments led us to compare the properties of reaction byproducts or intermediates obtained at early stages of milling to those observed in solution. For this, we monitored the reactions in the solid-state and in solution by ^{1}H NMR, Fourier-transform infrared attenuated total reflectance (FTIR-ATR) spectroscopy, and atomic force microscopy (AFM). In particular, we noticed that the ^{1}H NMR chemical shifts of the byproducts formed under milling conditions (Fig. 1a, *top*) were different from those of the solution self-assembly (Figure 1b, *top*), suggesting that these side-products or oligomers may be different. Similar results were obtained by comparing the FTIR-ATR spectra of the crude milled reaction mixture, which was consistent with that of the platinum(II) cationic square, and that of the solution reaction (after solvent evaporation, Supporting Information; section 11, Fig. S11 and S19).

We were interested to find out if the side-products formed in solution are intermediate oligomers that could be converted to the square upon milling.[14] After 90 minutes milling of the residue obtained from evaporation of the solution reaction under 3 days reflux, ^{1}H NMR spectroscopy did not reveal further square formation (Figure 1b, *bottom*). This indicates that the byproducts from the solution self-assembly are not equivalent to intermediates of the solid-state milling reaction, but may be off-pathway products that do not lead to the platinum(II) cationic square. Presumably, the solid-state reaction which occurs on a short timescale of minutes to hours would proceed *via* shorter oligomeric intermediate structures that quickly convert to the

square. In contrast, the solution-based reaction occurs at a much longer longer timescale and higher temperature, possibly leading to longer oligomeric structures that would be difficult to break down by milling into the tetrameric structures required for cyclization into the square. As a preliminary route to verify this, we carried out AFM studies of the pure square material, revealing uniform spherical structures with average height of 4.4 nm and diameter around 19 nm (Supporting information Figure S12). The AFM of a sample after 30 minutes milling shows a mostly monodisperse population of spherical structures very similar to that observed for the pure square, with average height 4.9 nm and width of 20.5 nm (Fig. 1c). On the other hand, AFM inspection of the solid sample obtained after 3 days aqueous reflux followed by evaporation revealed very different particle morphologies: here the spherical particles were significantly larger, with average height of 17 nm and width of 104 nm, indicating that the species obtained in solution are larger than the ones formed by milling (Fig. 1d). Solution self-assembly of platinum squares by heating for 3 days thus results in kinetic products that are large and oligomeric, and are difficult to break down to smaller species that could cyclize to the square. The entropic cost for these structures may be lower than that for the square formation, and the high reaction temperature would accentuate this difference.

Synthesis of Larger Squares **S2-S4**

The successful synthesis of a cationic platinum(II) square of **L1** by a two-step milling process starting from K_2PtCl_4 led us to explore whether the same reaction conditions would be applicable for the synthesis of square structures based on other bridging ligands, **L2-L4**. Notably, platinum squares based on these bridging ligands have not yet been described, with previous attempts in solution with palladium analogues leading to oligomers or other cyclic structures.[46] The mechanochemical reactions of **L2-L4** were found to be unexpectedly sensitive to the choice

of silver salt. Whereas poor conversions were observed with $AgNO_3$, as evidenced by ^{1}H NMR, excellent results were obtained with silver triflate, which might be due to templating effects that triflate anions were found to exhibit in syntheses of metalla-assemblies.[47] The use of AgO_3SCF_3 as the silver source enabled the first mechanochemical synthesis of the family of Pt(II) squares **S2-S4** (Scheme 1), demonstrating a general route for solvent-free, rapid synthesis of supramolecular squares, including those previously not attainable from solution, starting from the simple reagent K_2PtCl_4. The ^{1}H NMR yields for **S1-S4** were high (**S1**: 90%, **S2**: 80%, **S3**: 85% and **S4**: 75%), and Scheme 1 shows the isolated yields for each molecule.

The formation of these cationic platinum squares was established by ^{1}H NMR, IR and UV-vis spectroscopies, as well as by high-resolution mass spectrometry (Supporting Information; section 4 and 12). By ^{1}H NMR, downfield shifts were noted for the 4,4'-bipyridine ligand protons, and in the case of **S1**, these agreed with literature chemical shifts.[14,41] (Supporting information Figure S13). Diffusion-ordered NMR (DOSY) for **S1-S4** showed that proton signals of the same square have the same diffusion coefficient, which indicates the presence of only one species in solution. The diffusion coefficients of these systems in CD_3OD were comparable to those found for analogues,[48] and the rate of diffusion was found to scale with square size as expected, with the fastest diffusion for the smallest square (**S1**) (Fig. 3a). NOESY experiments confirmed the coordination of both **en** and **L1** to the platinum. (Supporting Information Figure S17 and S18). The formation of the platinum systems was further confirmed by high resolution electrospray ionization mass spectrometry (ESI-MS) (Figure 2b), which show a tri- and/or penta-cationic peak corresponding to the intact Pt(II)-squares.

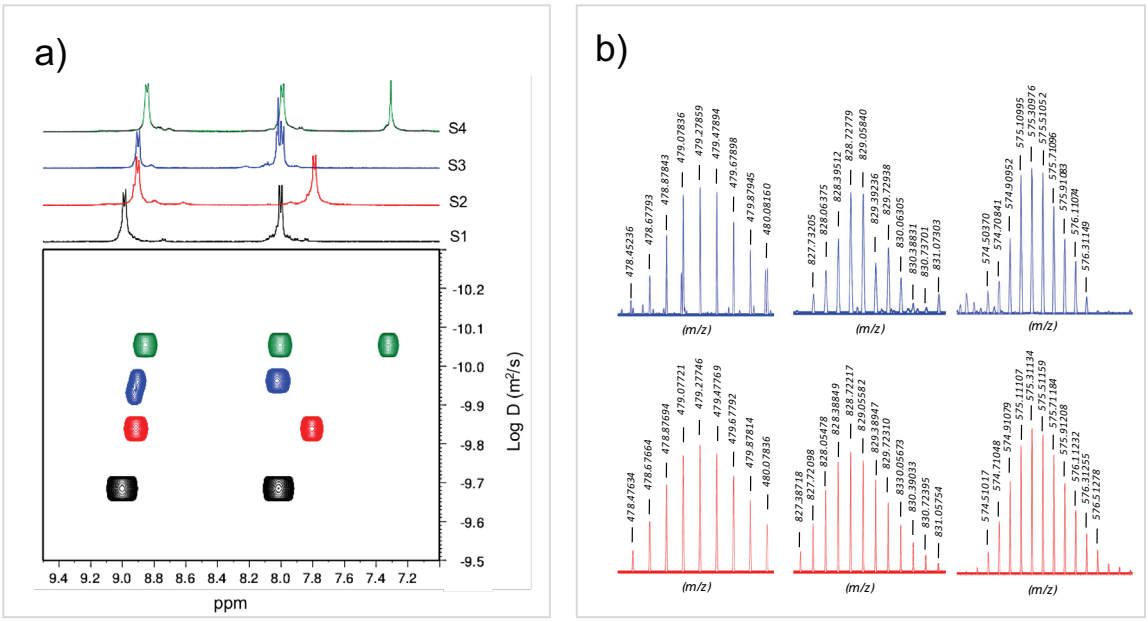

Figure 2 a) DOSY NMR spectra in (CD_3OD, 23 °C) of the Pt-squares (**S1-S4**); b) Selected ESI-MS peaks from the newly synthesized Pt-square **S3** (left), **S2** (middle) and **S4** (right) corresponding to the fragment ([**S3** + 3 CF_3SO_3]$^{5+}$), ([**S2** + 5 CF_3SO_3]$^{3+}$) and ([**S4** + 3 CF_3SO_3]$^{5+}$) respectively (top); Calculated ESI-MS peaks (bottom).

Dynamic Behavior of the Squares under Milling Conditions.

The inert nature of the Pt-N bond means that dynamic exchange of ligands in the squares **S1-S4** would be slow under ambient conditions. However, we were interested in probing whether this dynamic exchange can be accelerated in the solid state under milling conditions. Specifically, we (i) added a competing ligand to a platinum square assembly and analyzed the new species formed after milling, and (ii) we mixed two different platinum squares and probed any ligand exchange between them.[49]

When an excess of free 4,4'-bipyridine ligand was added to the square **S3** under milling conditions (milling at 25Hz for 90 min), dynamic exchange was observed. The square **S1** was formed in a 1:2 ratio compared to **S3**, and free **L3** was also detected, as evidenced by ^{1}H NMR, ^{1}H-COSY NMR and ^{1}H-DOSY NMR spectra (Figure 3). **S1** can possibly form by dissociation of square **S3** and binding of **L1**, or by an associative mechanism involving **S3** and ligand **L1**.[15,49a] While the DOSY experiment was consistent with a degree of self-sorting into **S1** and **S3**, it was

not clear whether mixed squares containing both **L1** and **L3** were also formed, due to the broad peaks observed. (Figure 3).

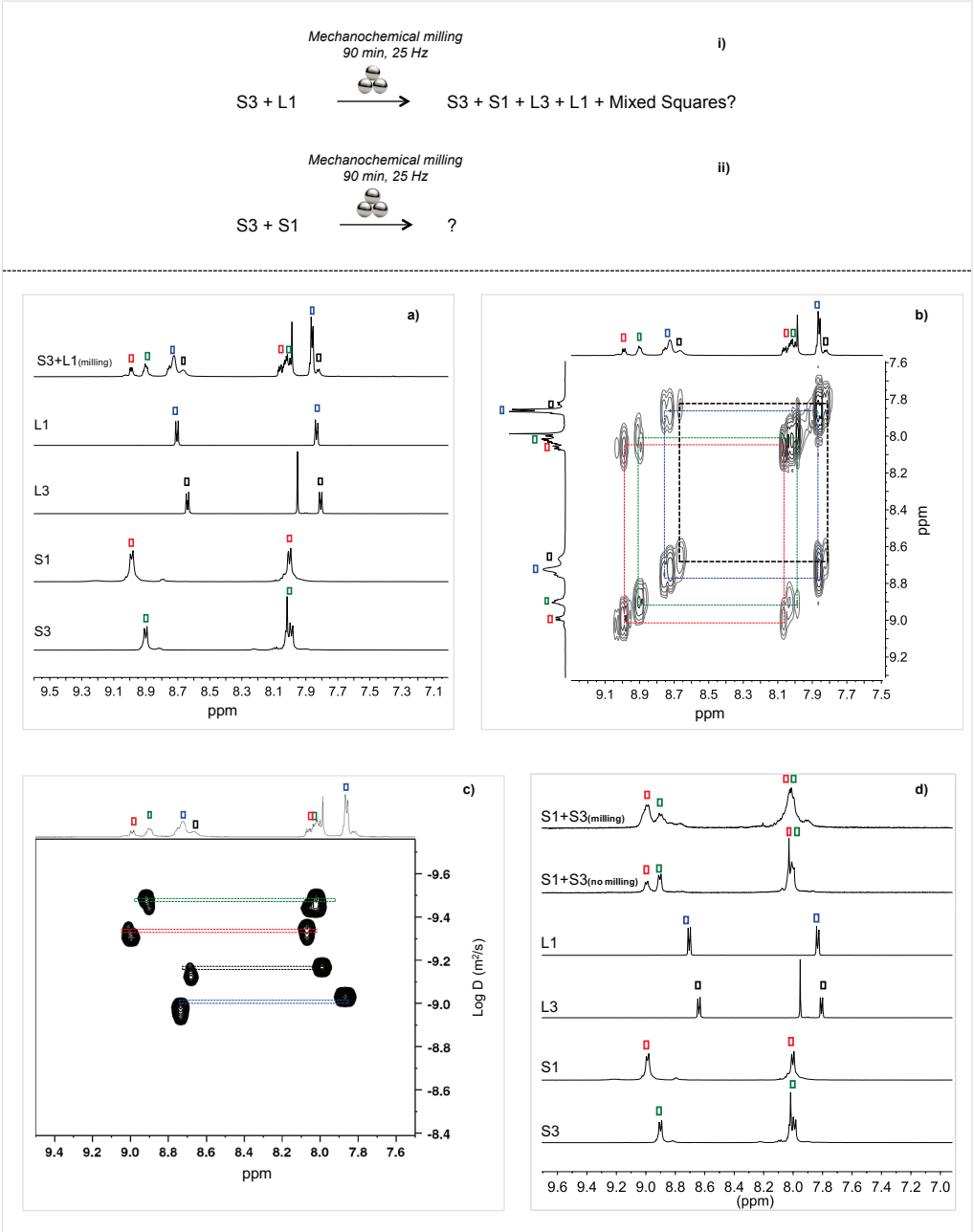

Figure 3 (top) Scheme of the reactions performed to probe dynamic exchange in the solid state under milling conditions, i) excess of free 4,4'-bipyridine ligand was added to the square **S3** under milling conditions (milling at 25Hz for 90 min); ii) A mixture of **S1** and **S3** squares in 1:1 molar ratio were also subjected to ball milling at 25 Hz for 30 min. (bottom) a) Representative ^{1}H NMR; b) ^{1}H-^{1}H COSY NMR; c) ^{1}H DOSY NMR spectra (CD_3OD, 23 °C) following the solid state ligand exchange process (milling for 30 min) with metallo-square $[Pt_4(en)_4(\mathbf{L_3})_4]^{8+}[CF_3SO_3]_8$ (**S3**) upon addition of 4,4'-bipyridine ligand (**L1**); d) ^{1}H NMR spectra (CD_3OD, 23 °C) following the solid state exchange process (milling for 30 min at 25 Hz) of a mixture of **S1** and **S3** squares in 1:1 molar ratio.

A mixture of **S1** and **S3** squares in 1:1 molar ratio were also subjected to ball milling at 25 Hz for 30 min. The signals were broadened, indicating possible dynamic ligand exchange between the two assemblies, albeit to a smaller extent than the exchange between square **S3** and ligand **L1** (Figure 3). The major signals associated with each square were found intact in ^{1}H NMR and ^{1}H-COSY NMR spectra (Figure 3). Signals associated with uncoordinated bipyridine ligands were absent.

In summary, we observed that: (i) rate acceleration by milling occurs in the solid state; (ii) self-assembly in solution requires heating and long reaction times, which results in the formation of much larger oligomeric by-products than the milling process, and these are difficult to convert back to the square complex; (iii) ball milling facilitates the exchange of ligand into a preformed square, and to a lesser extent, the dynamic exchange of two different squares.

Tentatively, we explain the observed acceleration of the rate of ligand exchange and square formation upon milling as a result of the very high concentration of reactants in the solid-state, thus accelerating associative second-order processes for platinum complexes. In contrast, solution processes involve a competitive solvent coordination process, which most likely dominates because of the high solvent concentration. Mechanochemical treatment has been shown to improve many fundamental organometallic reactions, including ligand exchange and oxidative addition.[42,50] In contrast, solvent coordination may block the platinum binding sites, thus requiring heating to replace with ligand. With heating and long reaction times, long oligomers form, and they are difficult to break down to smaller structures that would cyclize to the tetramer, and thus the self-assembly only partially yields the square in solution. [51]

Guanine Quadruplex Targeting

Libraries of platinum squares with different shape, size and functionalities would be a good basis to test structure-activity relationships with RNA and DNA G-quadruplexes.[40] **S2** is slightly larger than **S1** without introduction of steric bulk, and the phenyl group in **S3** aims at strengthening the π-π interactions properties with G-quadruplexes. The (hydroxyethoxy) vertex unit of **S4** can be used to provide multiple hydrogen-bonding interactions, which have been shown to increase RNA quadruplex binding affinity.[36a,36d,52] RNA specific ligands with available hydrogen bonding moieties interact with the hydroxyl group within RNA loops of the quadruplex, thus increasing stability and specificity.[36a,36c,36d,53]

In the present work, fluorescence intercalator displacement (FID), UV/vis binding titration and isothermal calorimetry assays were used to evaluate the binding affinity and specificity of the platinum squares to TERRA compared to telomeric and oncogene promoter G4s.[54] Here, one RNA and two DNA G-quadruplex-forming sequences were chosen: RNA TERRA corresponding to a single stranded fragment of human telomeric RNA overhang G-rich (UUAGGG) repeats (TERRA), H-telo corresponding to a fragment of the (TTAGGG) human telomeric repeats, KRAS consisting of a G-repeating sequence within the promoter of the KRAS gene, as well as double stranded sequence ds26mer and single stranded RNA sequence TERRA-mut used as control sequences (Supporting information Table S1).

The G4-FID assay involves binding the G-quadruplex samples to the probe thiazole orange (TO), which is highly fluorescent when bound to DNA and RNA sequences, but loses its fluorescence in the free state in aqueous medium. The addition of a stronger DNA binder (platinum square) to the TO-quadruplex structure causes the displacement of the dye, and hence, decreased fluorescence. (Figure 4)

The concentrations of platinum square required to give a 50 % decrease in dye fluorescence (DC_{50}) are shown in Table 1. The DC_{50} values for squares **S1-S4** showed strong binding to G-quadruplexes and were sub-micromolar for most complexes. In comparison to smaller monometallic complexes,[55] the platinum squares **S1-S4** showed lower DC_{50} values and faster binding (Supporting information Table S2), consistent with their increased positive charge and π-stacking surface.

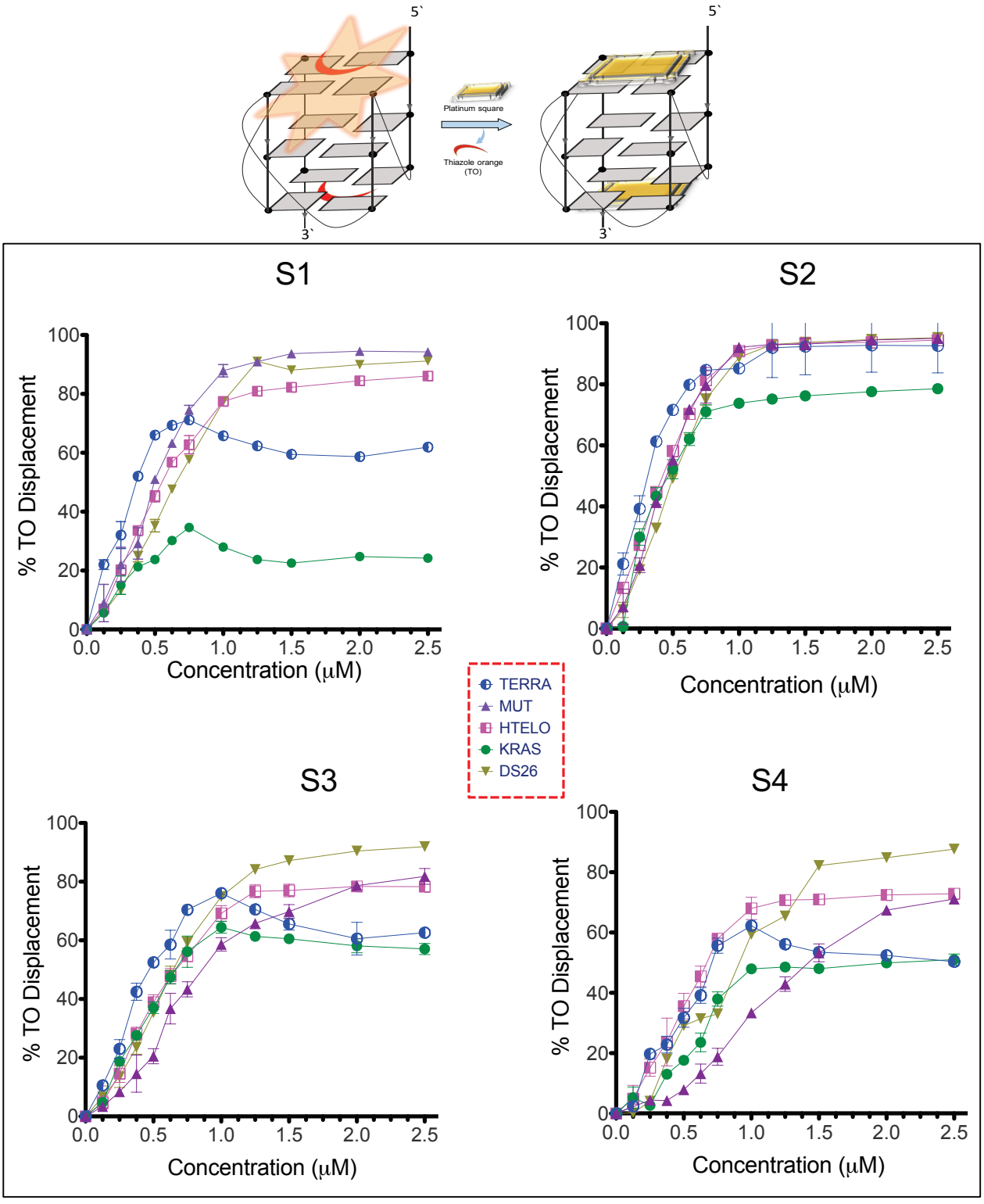

Figure 4. (top) Schematic of the competitive Fluorescence Displacement (FID) Assay. The thiazole orange dye (red crescent) is highly fluorescent when bound to the G-quadruplex motif. Addition of the G-quadruplex ligand (platinum square) leads to the displacement of the dye and decrease of the sample fluorescence. (bottom) FID data obtained for the squares **S1-S4**.

Table 1. *DC_{50} values [μM] for S1–S4 (90 min incubation), as determined by FID assay.*

Oligonucleotide	***S1***	***S2***	***S3***	***S4***
TERRA	0.352	0.253	0.426	0.727
TERRA-mut	0.533	0.415	0.901	1.41
H-telo	0.533	0.403	0.641	0.66
KRAS	>2.5	0.446	0.666	1.21
ds26mer	0.669	0.505	0.641	0.927

In general, squares **S1-S3** bound better to TERRA than to other G-quadruplex sequences, with **S2** being the strongest binder, while **S4** had a stronger affinity to H-telo. For the TERRA G4 motif, the squares showed a strong affinity with DC_{50} values varying from 0.727 (**S4**) to 0.253 μM (**S2**). The selectivities for TERRA vs. the non-quadruplex DNA structure TERRA-mut were modest (DC_{50} (TERRA)/ DC_{50} (TERRA-mut) = 0.66, 0.61, 0.47, 0.51) with **S3** as the most selective. This is consistent with the high positive charge of the platinum squares (+8). However, the facile and efficient mechanochemical synthesis introduced here will allow the generation of libraries of self-assembled platinum complexes with lower charge and greater selectivity.

The FID results were confirmed by UV/vis binding titrations of the squares **S2** and **S3**, which showed demonstrated a red shift and a mild hypochromicity of the bands at ~ 300 nm (Supporting Information Figure S1), providing evidence for a π-stacking binding mode.

As a means of obtaining further thermodynamic insight into the interaction of **S1** with the TERRA, TERRA-mut and H-telo sequences, isothermal titration calorimetry experiments were performed. **S1** showed a standard sigmoidal binding isotherm to the TERRA sequence, while the TERRA-mut and H-telo had more complex profiles (Supporting information Figure S25). The

TERRA binding profile was fit using a single binding site model while the other isotherms were fit using the sequential binding sites model using 3 and 4 sites for TERRA-mut and H-telo respectively. This complex binding behavior has been previously reported for the interactions between Pt (II) squares and telomeric G-quadruplexes.[56] The thermodynamic parameters that could be accurately extracted are summarized in Table 2, and the remainder of the fitted terms can be found in the Supporting Information Figure S25. Importantly, the K_ds extracted using ITC (0.42 μM, 0.9 μM, and 2.2 μM for TERRA, TERRA-mut, and H-telo respectively) are in agreement with the DC_{50} obtained via FID. Interestingly, the number of sites differs for each sequence; TERRA shows a ~2:1 (1.72:1) **S1**:oligonucleotide stoichiometry, while the TERRA-mut and H-telo sequences appear to bind **3** and **4 S1** ligands per quadruplex respectively. Furthermore, the total enthalpy of binding (the sum of all the individual enthalpic terms from the fits) is negative for the interaction with all oligonucleotides indicating that the overall process is enthalpically favorable. Overall, the ITC results help by benchmarking the parameters extracted from the FID and provide a small window of insight into the complex binding mechanisms for these systems.

Table 2. *Summary of thermodynamic parameters obtained by isothermal calorimetry.*

Oligonucleotide	n	K_d (10^{-6} M)	ΔH (kcalmol^{-1})	TΔS (kcalmol^{-1})
TERRA	1.72±0.02	0.403 ± 0.052	-5.00 ± 0.94	3.73 ± 0.46
TERRA-mut	3	0.943 ± 0.133	-8.35 ± 0.25	0.15 ± 0.02
H-telo	4	2.22 ± 0.32	-11.1 ± 0.7	-3.37 ± 0.49

In conclusion, we have shown a rapid and efficient synthesis of therapeutically interesting supramolecular platinum squares from the readily available precursor K_2PtCl_4 using mechanochemical ball milling. While solution-based assembly of these structures requires refluxing for days (weeks) and gives lower yields, ball milling gives the squares at room temperature, in minutes and in good to excellent yields. We carried out several experiments to gain mechanistic insight into this remarkable rate acceleration. These revealed that the long reaction time and high temperatures required by the solution conditions result in the formation of large oligomeric side-products, which are difficult to break down into the square. In contrast, the high concentration of reactants in the solid-state accelerates the associative processes that produce the platinum square, without resulting in off-pathway products. Mechanochemical treatment was also found to accelerate the dynamic exchange of the squares with other added ligands.

Using this method, we synthesized previously unreported platinum squares and examined their binding to DNA and RNA guanine quadruplexes. These included telomere associated DNA and RNA sequences as well as oncogene sequences. These squares showed submicromolar binding affinities to the RNA telomeric sequence TERRA, which regulates telomere elongation in both telomerase positive and telomerase negative (ALT) cancer cells. We believe that the herein presented facile synthesis of inert metallosupramolecular squares will enable the rapid optimization of their binding selectivity and therapeutic potential. We are currently looking into expanding solid-state ball milling reactions to other, more complex self-assembling systems, particularly those those based on kinetically inert bonds.

Acknowledgments

The authors would like to thank NSERC, CIHR, CFI, the Canada Research Chairs Program, FQRNT and CSACS for funding.

Associated content

Supporting information: synthetic procedures, spectroscopic and microscopy characterization.

Author information

Co-corresponding authors *tomislav.friscic@mcgill.ca *hanadi.sleiman@mcgill.ca

References

(1) a. Cook, T. R.; Stang, P. J. *Chem. Rev.* **2015**, *115*, 7001-7045; b. Cook, T. R.; Vajpayee, V.; Lee, M. H.; Stang, P. J.; Chi, K.-W. *Acc. Chem. Res.* **2013**, *46*, 2464–2474; c. McConnell, A. J.; Wood, C. S.; Neelakandan, P. P.; Nitschke, J. R. *Chem. Rev.* **2015**, *115*, 7729-7793; d. Therrien, B. *Chem. Eur. J.* **2013**, *19*, 8378-8386; e. Garci, A.; Mbakidi, J.-P.; Chaleix, V.; Sol, V.; Orhan, E.; Therrien, B. *Organometallics* **2015**, *34*, 4138-4146; f. Garci, A.; Dobrov, A. A.; Riedel, T.; Orhan, E.; Dyson, P. J.; Arion, V. B.; Therrien, B. *Organometallics* **2014**, *33*, 3813-3822.

(2) a. Dalgarno, S. J.; Power, N. P.; Atwood, J. L. *Coord. Chem. Rev.* **2008**, *252*, 825-841; b. Chakrabarty, R.; Mukherjee, P. S.; Stang, P. J. *Chem. Rev.* **2011**, *111*, 6810-6918; c. Mukherjee, S.; Mukherjee, P. S. *Chem. Comm.* **2014**, *50*, 2239-2248.

(3) a. Fujita, M.; Ibukuro, F.; Hagihara, H.; Ogura, K. *Nature* **1994**, *367*, 720-723; b. Ibukuro, F.; Kusukawa, T.; Fujita, M. *J. Am. Chem. Soc.* **1998**, *120*, 8561-8562; c. Roche, S.; Haslam, C.; L. Heath, S.; A. Thomas, J. *Chem. Comm.* **1998**, 1681-1682; d. Xie, T.-Z.; Liao, S.-Y.; Guo, K.; Lu, X.; Dong, X.; Huang, M.; Moorefield, C. N.; Cheng, S. Z. D.; Liu, X.; Wesdemiotis, C.; Newkome, G. R. *J. Am. Chem. Soc.* **2014**, *136*, 8165-8168.

(4) Vivekananda, K. V.; Dey, S.; Maity, D. K.; Bhuvanesh, N.; Jain, V. K. *Inorg. Chem.* **2015**, *54*, 10153-10162.

(5) Zhang, M.; Saha, M. L.; Wang, M.; Zhou, Z.; Song, B.; Lu, C.; Yan, X.; Li, X.; Huang, F.; Yin, S.; Stang, P. J. *J. Am. Chem. Soc.* **2017**, *139*, 5067-5074.

(6) a. Grishagin, I. V.; Pollock, J. B.; Kushal, S.; Cook, T. R.; Stang, P. J.; Olenyuk, B. Z. *P. Natl. Acad. Sci. USA* **2014**, *111*, 18448-18453; b. Zhang, M. M.; Li, S. Y.; Yan, X. Z.; Zhou, Z. X.; Saha, M. L.; Wang, Y. C.; Stang, P. J. *P. Natl. Acad. Sci. USA* **2016**, *113*, 11100-11105.

(7) Zheng, Y.-R.; Suntharalingam, K.; Johnstone, T. C.; Lippard, S. J. In *Chem. Sci.* 2015; Vol. 6, p 1189-1193.

(8) Fyles, T. M.; Tong, C. C. *New J. Chem.* **2007**, *31*, 655-661.

(9) a. Bivaud, S.; Balandier, J. Y.; Chas, M.; Allain, M.; Goeb, S.; Salle, M. *J. Am. Chem. Soc.* **2012**, *134*, 11968-11970; b. Croue, V.; Goeb, S.; Szaloki, G.; Allain, M.; Salle, M. *Angew. Chem. Int. Ed.* **2016**, *55*, 1746-1750.

(10) Fujita, M.; Yazaki, J.; Ogura, K. *J. Am. Chem. Soc.* **1990**, *112*, 5645-5647.

(11) Kieltyka, R.; Englebienne, P.; Fakhoury, J.; Autexier, C.; Moitessier, N.; Sleiman, H. F. *J. Am. Chem. Soc.* **2008**, *130*, 10040-10041.

(12) Fujita, M.; Tominaga, M.; Hori, A.; Therrien, B. *Acc. Chem. Res.* **2005**, *38*, 369-378.

(13) a. Kuehl, C. J.; Mayne, C. L.; Arif, A. M.; Stang, P. J. *Org. Lett.* **2000**, *2*, 3727-3729; b. Kuehl, C. J.; Huang, S. D.; Stang, P. J. *J. Am. Chem. Soc.* **2001**, *123*, 9634-9641.

(14) Fujita, M.; Ibukuro, F.; Yamaguchi, K.; Ogura, K. *J. Am. Chem. Soc.* **1995**, *117*, 4175-4176.

(15) Yamashita, K.-i.; Kawano, M.; Fujita, M. *J. Am. Chem. Soc.* **2007**, *129*, 1850-1851.

(16) a. Yamashita, K.-i.; Sato, K.-i.; Kawano, M.; Fujita, M. *New J. Chem.* **2009**, *33*, 264-270; b. Symmers, P. R.; Burke, M. J.; August, D. P.; Thomson, P. I. T.; Nichol, G. S.; Warren, M. R.; Campbell, C. J.; Lusby, P. J. *Chem. Sci.* **2015**, *6*, 756-760; c. Burke, M. J.; Nichol, G. S.; Lusby, P. J. *J. Am. Chem. Soc.* **2016**, *138*, 9308-9315.

(17) a. Li, Z.-Q.; Qiu, L.-G.; Wang, W.; Xu, T.; Wu, Y.; Jiang, X. *Inorg. Chem. Commun.* **2008**, *11*, 1375-1377; b. Xiao, J.-D.; Qiu, L.-G.; Ke, F.; Yuan, Y.-P.; Xu, G.-S.; Wang, Y.-M.; Jiang, X. *J. Mat. Chem. A* **2013**, *1*, 8745-8752.

(18) López-Vidal, E. M.; Blanco, V.; García, M. D.; Peinador, C.; Quintela, J. M. *Org. Lett.* **2012**, *14*, 580-583.

(19) Friscic, T. *Chem. Soc. Rev.* **2012**, *41*, 3493-3510.

(20) Cliffe, M. J.; Mottillo, C.; Stein, R. S.; Bucar, D.-K.; Friscic, T. *Chem. Sci.* **2012**, *3*, 2495-2500.

(21) a. James, S. L.; Adams, C. J.; Bolm, C.; Braga, D.; Collier, P.; Friscic, T.; Grepioni, F.; Harris, K. D. M.; Hyett, G.; Jones, W.; Krebs, A.; Mack, J.; Maini, L.; Orpen, A. G.; Parkin, I. P.; Shearouse, W. C.; Steed, J. W.; Waddell, D. C. *Chem. Soc. Rev.* **2012**, *41*, 413-447; b. Garay, A. L.; Pichon, A.; James, S. L. *Chem. Soc. Rev.* **2007**, *36*, 846-855; c. Boldyreva, E. *Chem. Soc. Rev.* **2013**, *42*, 7719-7738; d. Rightmire, N. R.; Hanusa, T. P. *Dalton Trans.* **2016**, *45*, 2352-2362.

(22) a. Szymański, M.; Wierzbicki, M.; Gilski, M.; Jędrzejewska, H.; Sztylko, M.; Cmoch, P.; Shkurenko, A.; Jaskólski, M.; Szumna, A. *Chem. Eur. J.* **2016**, *22*, 3148-3155; b. Sokolov, A. N.; Bučar, D.-K.; Baltrusaitis, J.; Gu, S. X.; MacGillivray, L. R. *Angew. Chem. In. Ed.* **2010**, *49*, 4273-4277.

(23) a. Braga, D.; Giaffreda, S. L.; Grepioni, F.; Pettersen, A.; Maini, L.; Curzi, M.; Polito, M. *Dalton Trans.* **2006**, 1249-1263; b. Delori, A.; Friscic, T.; Jones, W. *CrystEngComm* **2012**, *14*, 2350-2362.

(24) Cinčić, D.; Friščić, T.; Jones, W. *J. Am. Chem. Soc.* **2008**, *130*, 7524-7525.

(25) a. Belenguer, A. M.; Lampronti, G. I.; Wales, D. J.; Sanders, J. K. M. *J. Am. Chem. Soc.* **2014**, *136*, 16156-16166; b. Biswal, B. P.; Chandra, S.; Kandambeth, S.; Lukose, B.; Heine, T.; Banerjee, R. *J. Am. Chem. Soc.* **2013**, *135*, 5328-5331.

(26) a. Mottillo, C.; Friscic, T. *Molecules* **2017**, *22*; b. Julien, P. A.; Mottillo, C.; Friscic, T. *Green Chem.* **2017**, *19*, 2729-2747.

(27) Akimbekov, Z.; Katsenis, A. D.; Nagabhushana, G. P.; Ayoub, G.; Arhangelskis, M.; Morris, A. J.; Friščić, T.; Navrotsky, A. *J. Am. Chem. Soc.* **2017**, *139*, 7952-7957.

(28) a. Karki, S.; Friscic, T.; Jones, W. *CrystEngComm* **2009**, *11*, 470-481; b. Weyna, D. R.; Shattock, T.; Vishweshwar, P.; Zaworotko, M. J. *Cryst. Growth Des.* **2009**, *9*, 1106-1123.

(29) Giri, C.; Sahoo, P. K.; Puttreddy, R.; Rissanen, K.; Mal, P. *Chem. Eur. J.* **2015**, *21*, 6390-6393.

(30) Cheung, E. Y.; Kitchin, S. J.; Harris, K. D. M.; Imai, Y.; Tajima, N.; Kuroda, R. *J. Am. Chem. Soc.* **2003**, *125*, 14658-14659.

(31) Atwood, J. L.; Hardie, M. J.; Raston, C. L.; Sandoval, C. A. *Org. Lett.* **1999**, *1*, 1523-1526.

(32) Antesberger, J.; Cave, G. W. V.; Ferrarelli, M. C.; Heaven, M. W.; Raston, C. L.; Atwood, J. L. *Chem. Comm.* **2005**, 892-894.

(33) Içli, B.; Christinat, N.; Tönnemann, J.; Schüttler, C.; Scopelliti, R.; Severin, K. *J. Am. Chem. Soc.* **2009**, *131*, 3154-3155.

(34) a. Neidle, S. *J. Med. Chem.* **2016**, *59*, 5987-6011; b. Neidle, S. **2017**, *1*, 0041; c. Kieltyka, R.; Fakhoury, J.; Moitessier, N.; Sleiman, H. F. *Chem. Eur. J.* **2008**, *14*, 1145-1154; d. Autexier, C.; Brault, M. E.; Englebienne, P.; Fakhoury, J.; Kieltyka, R.; Moitessier, N.; Sleiman, H. *Anticancer Res* **2008**, *28*, 3201-3202; e. Mancini, J.; Rousseau, P.; Castor, K. J.; Sleiman, H. F.; Autexier, C. *Biochimie* **2016**, *121*, 287-297.

(35) Xu, Y. *Chem. Soc. Rev.* **2011**, *40*, 2719-2740.

(36) a. Di Antonio, M.; Biffi, G.; Mariani, A.; Raiber, E. A.; Rodriguez, R.; Balasubramanian, S. *Angew. Chem. Int. Ed.* **2012**, *51*, 11073-8; b. Garavis, M.; Lopez-Mendez, B.; Somoza, A.; Oyarzabal, J.; Dalvit, C.; Villasante, A.; Campos-Olivas, R.; Gonzalez, C. *ACS Chem Biol* **2014**, *9*, 1559-66; c. Katsuda, Y.; Sato, S.; Asano, L.; Morimura, Y.; Furuta, T.; Sugiyama, H.; Hagihara, M.; Uesugi, M. *J. Am. Chem. Soc.* **2016**, *138*, 9037-40; d. Collie, G.; Reszka, A. P.; Haider, S. M.; Gabelica, V.; Parkinson, G. N.; Neidle, S. *Chem. Comm.* **2009**, 7482-4.

(37) a. Cao, Q.; Li, Y.; Freisinger, E.; Qin, P. Z.; Sigel, R. K. O.; Mao, Z.-W. *Inorg. Chem. Front.* **2017**, *4*, 10-32; b. Rouleau, S.; Jodoin, R.; Garant, J.-M.; Perreault, J.-P.; RNA G-Quadruplexes as Key Motifs of the Transcriptome; Springer Heidelberg, p 1-20.

(38) Zheng, X.-H.; Chen, H.-Y.; Tong, M.-L.; Ji, L.-N.; Mao, Z.-W. *Chem. Comm.* **2012**, *48*, 7607-7609.

(39) Zheng, X.-H.; Zhong, Y.-F.; Tan, C.-P.; Ji, L.-N.; Mao, Z.-W. *Dalton Trans.* **2012**, *41*, 11807-11812.

(40) Domarco, O.; Lotsch, D.; Schreiber, J.; Dinhof, C.; Van Schoonhoven, S.; Garcia, M. D.; Peinador, C.; Keppler, B. K.; Berger, W.; Terenzi, A. *Dalton Trans.* **2017**, *46*, 329-332.

(41) Orita, A.; Jiang, L.; Nakano, T.; Ma, N.; Otera, J. *Chem. Comm.* **2002**, 1362-1363.

(42) Hernandez, J. G.; Butler, I. S.; Friscic, T. *Chem Sci* **2014**, *5*, 3576-3582.

(43) Ferguson, M.; Giri, N.; Huang, X.; Apperley, D.; James, S. L. *Green Chem.* **2014**, *16*, 1374-1382.

(44) Balaz, P.; Achimovicova, M.; Balaz, M.; Billik, P.; Cherkezova-Zheleva, Z.; Criado, J. M.; Delogu, F.; Dutkova, E.; Gaffet, E.; Gotor, F. J.; Kumar, R.; Mitov, I.; Rojac, T.; Senna, M.; Streletskii, A.; Wieczorek-Ciurowa, K. *Chem. Soc. Rev.* **2013**, *42*, 7571-7637.

(45) a. Do, J.-L.; Friščić, T. *ACS Cent. Sci.* **2017**, *3*, 13-19; b. Friscic, T.; Childs, S. L.; Rizvi, S. A. A.; Jones, W. *CrystEngComm* **2009**, *11*, 418-426.

(46) Uehara, K.; Kasai, K.; Mizuno, N. *Inorg. Chem.* **2010**, *49*, 2008-2015.

(47) Duchêne, D.; Gref, R. *Int. J. Pharmac.* **2016**, *502*, 219-231.

(48) a. Ferrer, M.; Gutiérrez, A.; Mounir, M.; Rossell, O.; Ruiz, E.; Rang, A.; Engeser, M. *Inorg. Chem.* **2007**, *46*, 3395-3406; b. Ferrer, M.; Pedrosa, A.; Rodríguez, L.; Rossell, O.; Vilaseca, M. *Inorg. Chem.* **2010**, *49*, 9438-9449.

(49) a. Zheng, Y.-R.; Stang, P. J. *J. Am. Chem. Soc.* **2009**, *131*, 3487-3489; b. Li, J.-R.; Zhou, H.-C. *Nat. Chem.* **2010**, *2*, 893-898; c. Garci, A.; Marti, S.; Schurch, S.; Therrien, B. *RSC Adv.* **2014**, *4*, 8597-8604.

(50) Hernandez, J. G.; Macdonald, N. A. J.; Mottillo, C.; Butler, I. S.; Friscic, T. *Green Chem.* **2014**, *16*, 1087-1092.

(51) Rightmire, N. R.; Hanusa, T. P.; Rheingold, A. L. *Organometallics* **2014**, *33*, 5952-5955.

(52) Koirala, D.; Dhakal, S.; Ashbridge, B.; Sannohe, Y.; Rodriguez, R.; Sugiyama, H.; Balasubramanian, S.; Mao, H. *Nat. Chem.* **2011**, *3*, 782-7.

(53) Takahama, K.; Miyawaki, A.; Shitara, T.; Mitsuya, K.; Morikawa, M.; Hagihara, M.; Kino, K.; Yamamoto, A.; Oyoshi, T. *ACS Chem Biol* **2015**, *10*, 2564-9.

(54) a. Monchaud, D.; Allain, C.; Bertrand, H.; Smargiasso, N.; Rosu, F.; Gabelica, V.; De Cian, A.; Mergny, J. L.; Teulade-Fichou, M. P. *Biochimie* **2008**, *90*, 1207-1223; b. Mergny, J.-L.; De Cian, A.; Ghelab, A.; Saccà, B.; Lacroix, L. *Nucl. Acids. Res.* **2005**, *33*, 81-94.

(55) a. Castor, K. J.; Mancini, J.; Fakhoury, J.; Weill, N.; Kieltyka, R.; Englebienne, P.; Avakyan, N.; Mittermaier, A.; Autexier, C.; Moitessier, N.; Sleiman, H. F. *Chemmedchem* **2012**, *7*, 85-94; b. Castor, K. J.; Liu, Z.; Fakhoury, J.; Hancock, M. A.; Mittermaier, A.; Moitessier, N.; Sleiman, H. F. *Chem. Eur. J.* **2013**, *19*, 17836-17845.

(56) a. Zheng, X. H.; Chen, H. Y.; Tong, M. L.; Ji, L. N.; Mao, Z. W. *Chem. Comm.* **2012**, *48*, 7607-9; b. Zheng, X. H.; Zhong, Y. F.; Tan, C. P.; Ji, L. N.; Mao, Z. W. *Dalton Trans.* **2012**, *41*, 11807-12.